



ARTICLE

# Non-linearity Analysis of Ship Roll Gyro-stabilizer Control System

Sathit P.<sup>1\*</sup> Chatchapol C.<sup>2</sup> Phansak I.<sup>3</sup>

1. Department of Maritime Engineering, Faculty of International Maritime Studies, Kasetsart University, Chonburi, 20230, Thailand

2. Department of Mechanical Engineering, Faculty of Engineering, Kasetsart University, Bangkok, 10900, Thailand

3. Department of Nautical Science and Maritime Logistics, Faculty of International Maritime Studies, Kasetsart University, Chonburi, 20230, Thailand

ARTICLE INFO

*Article history*

Received: 19 January 2021

Accepted: 24 May 2021

Published Online: 30 May 2021

*Keywords:*

Active gyro-stabilizer

Twin gyro-stabilizer

Ship large roll motion

System identification

Inverse problems

Non-linear damping moment

Non-linear restoring moment

ABSTRACT

A gyro-stabilizer is the interesting system that it can apply to marine vessels for diminishes roll motion. Today it has potentially light weight with no hydrodynamics drag and effective at zero forward speed. The twin-gyroscope was chosen. Almost, the modelling for designing the system use linear model that it might not comprehensive mission requirement such as high sea condition. The non-linearity analysis was proved by comparison the results between linear and non-linear model of gyro-stabilizer throughout frequency domain also same wave input, constrains and limitations. Moreover, they were cross checked by simulating in time domain. The comparison of interested of linear and non-linear close loop model in frequency domain has demonstrated the similar characteristics but gave different values at same frequency obviously. The results were confirmed again by simulation in irregular beam sea on time domain and they demonstrate the difference of behavior of both systems while the gyro-stabilizers are switching on and off. From the resulting analysis, the non-linear gyro-stabilizer model gives more real results that correspond to more accuracy in a designing gyro-stabilizer control system for various amplitudes and frequencies operating condition especially high sea condition.

## 1. Introduction

Of the six modes of motions of marine vessel, roll motion is the important mode to be realized. It is the greatest reason to capsize also affect to operation of crews, passengers comfortable and cargos damage, when a vessel is excited by wave load at high sea. In order to diminish amplitude of roll motion, roll stabilizer system becomes an important role.

More than 100 years, many types of roll stabilizer have been engineered by many researchers and designer. The following example, bilge keels, sloshing, sliding weight,

gyro, u-tube, sea-ducted, variable angle fins, hydro-foil keel fin and rotating cylinder etc.

Since 1995, Chadwick<sup>[1]</sup> had gathered types of roll stabilizers and it has been classified by control method to be passive and active control. The passive control is the control system does not require any external power source to operate the control device but the active control system does opposite way<sup>[2]</sup>. Some types of stabilizer are only passive control as bilge keels and sloshing. Some types are only active control such as variable angle fins and rotating cylinder. And some types are both as sliding weight,

\*Corresponding Author:

Sathit P.,

Department of Maritime Engineering, Faculty of International Maritime Studies, Kasetsart University, Chonburi, 20230, Thailand;

Email: [sathit.pon@ku.th](mailto:sathit.pon@ku.th)

u-tube, sea-ducted and gyro.

Another way, Haghighi and Jahed-Motlagh<sup>[3]</sup> have mentioned classification of system control types that can be classified as either external or internal control systems. The external control system is systems generate resisting load (forces and moments) outside a ship hull and the internal control system is systems generate resisting load inside<sup>[4]</sup>. The principal advantages of internal systems are not hydrodynamic drag and effective zero forward but it has heavyweight, volume penalty and there are limited in stabilisation capability. The external systems have lightweight but it creates hydrodynamic drag and ineffective at zero forward speed<sup>[5,6]</sup>. The following above mention and nowadays technology, a gyro-stabilizer become to be an interesting system at present. Because it has a combination of internal and external control system advantages: potentially light weight with no hydrodynamic drag and is effective at zero forward speed.

A gyro-stabilizer system is to use resisting moments, which moments are the cross product between angular momentum vector of flywheel and angular velocity vector around precession axis. The resisting moment is applied to vehicle or other to resist external excitation moments that are keeping minimal oscillatory amplitude of rolling vehicle. However, this paper focus on a gyro-stabilizer is applied to small ships.

Background stories of gyro-stabilizers, it has been applied to various inventions. The first gyro-stabilizer application was invented by Brennan<sup>[7]</sup>. Brennan used twin gyro that it had counter-rotating flywheels to stabilize unstable vehicle (two-wheel monorail car). This invention had similar patents<sup>[8,9,10]</sup>. More researches, gyro-stabilizers were applied to stabilize to two-wheel vehicles such as a bicycle<sup>[11]</sup> and motorcycles<sup>[12]</sup>. In 1996, Brown and his team published about the using gyro-stabilizer that provides mechanical stabilization and steering a single-wheel robot<sup>[13]</sup>. Another field, NASA used the advantage of gyro-stabilizer to control attitude of large space structures or satellite<sup>[14]</sup>. In additional, gyro-stabilizers have been applied to maritime field, e.g., autonomous under water vehicle<sup>[15,16]</sup>, torpedo<sup>[17]</sup> and free surface vehicle etc. The first record of a gyro-stabilizer in marine vehicles was found accidentally, Howell torpedo, it was installed rapid rotation of fly-wheel. There was 16 inches a steel wheel diameter and was spun up to 16,000 rpm. The torpedo was experimented for locking target on U.S. Navy boat<sup>[17]</sup>. For the first time of free surface vehicle, a gyro-stabilizer device was passive system that it was utilized to diminish roll motion<sup>[18,19,20]</sup>. Active gyro-stabilizer systems were developed from passive systems. The first system was proposed by Elmer Sperry in 1908<sup>[21]</sup>.

Recently, many researchers have proposed related new

researches of gyro-stabilizer with novel control methods. Townsend et al.<sup>[4]</sup> published a new active gyrostabiliser system for ride control of marine vehicle. McGookin et al.<sup>[22]</sup> published application of MPC and sliding mode control to IFAC benchmark models. Perez and Steinmann<sup>[23]</sup> demonstrated analysis of ship roll gyrostabilizer control that revisited the modelling of coupled vessel-gyrostabilizer and also describes design trade-offs under performance limitation. Haghighi and Jahed-Motlagh<sup>[3]</sup> proposed ship roll stabilization via sliding mode control and gyrostabilizer.

For designing ship roll gyro-stabilizers, a preliminary design is important thing. In order to design it, designers need to know wave loads, ship motion (ship model) and actuator characteristics (gyro-stabilizer model). Almost, modelling of designing uses an equation of motion in linear model that it may not comprehensive mission requirement, such as large roll motion from both high amplitudes and frequencies of waves. Normally, these have to be non-linear model under limitations that have more correction and accuracy also failure cases from system instability. The failure cases may not occur in linear modelling but it was found in non-linear. From these reasons, it becomes the motivation of this study. Both linear and non-linear model of gyro-stabilizer and ship were concerned.

Non-linear system modelling of gyro-stabilizer was comprised of ship rolling model and single axis gimbal gyroscope model (non-linear equation of motion). Normally, non-linearity of gyro-stabilizer model appears in restoring term and exciting moment term. However non-linearity of ship roll model able to appear all terms of equation of motion (term of inertia, damping, restoring and exciting moment).

In order to formulate non-linear ship roll model, the system identification method is used to find non-linear coefficients of added inertia, damping and restoring term of ship. The system identification methods of ship roll motion can be found in many papers such as Masri et al. (1993)<sup>[24]</sup>, Chassiakos and Marsi (1996)<sup>[25]</sup>, Liang et al. (1997)<sup>[26]</sup>, Liang et al. (2001)<sup>[27]</sup>, Jang et al. (2009)<sup>[28]</sup>, Jang et al. (2010)<sup>[29]</sup>, Jang (2011)<sup>[30]</sup> and Jang et al. (2011)<sup>[31]</sup> etc. However, in this paper uses method of Pongdung et al.<sup>[32]</sup> which is the novel method and able to find all of non-linear terms of ship model.

The objective of this presentation is to analyse non-linearity of ship roll twin gyro-stabilizer control system under limitations of wave load and precession angle via frequency domain analysis and time domain simulation.

## 2. Principals and Theories

Analysis of gyro-stabilizer system has three parts that is realised. It comprised of water wave model, ship

model and gyro-stabilizer model. In order to reach the present objective, the regular and irregular deep water wave models are selected to set simulation cases. The ship and gyro-stabilizer models is concerned both linear and non-linear model to observe and analyze effects of system non-linearity from simulation results.

The general principle of gyroscopic stabilization, its torque is produced by gyro-stabilizer that installed in a ship opposes roll exciting moment from water wave. This exciting moment disturbs the angular momentum of flywheel such that develops precession motion. The cross product of flywheel angular momentum and precession rate induces moment to resist the exciting moment in opposite direction [33]. Figure 1 explains working principle of gyro-stabilizer that is installed in a marine vessel. At present, twin-flywheels are selected, and there are spinning and precession angle rotate in opposite direction. Its result cancels the side effect of gyroscopic moments in the other directions (normally in pitch and yaw of ship). Figure 2 displays the working of twin gyro-stabilizer.

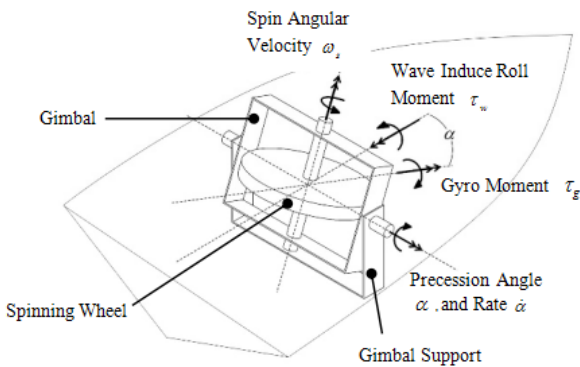


Figure 1. Illustration single gyro-stabilizer installation and its working principle

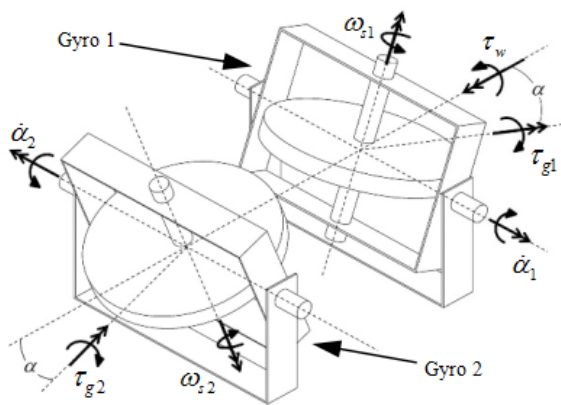


Figure 2. Demonstration working principle of twin gyro-stabilizer and elimination of its side effect of gyro-stabilisation moment

## 2.1 Full Non-linear Gyro-stabilizer Model

The prediction of gyro-stabilizer performances was modelled via the two equations of motions. The first equation is the ship model and the second equation is gyro-stabilizer model.

Consideration a ship motion, while it is excited by water wave that is demonstrated in Figure 3. Instantaneous, the ship is rolled by moment of inertia in counter clockwise and is acted by wave, which wave free surface has  $\beta$  (wave slope angle) against horizontal line. The  $y$  axis of body fix frame has  $\phi$  (roll angle) against horizontal line. Thus  $\theta$  is relative angle between roll and wave slope angle. The following Newton's second law, the equation of motion of ship can be written as

$$(I_{44} + I_{44a}(\ddot{\theta}))\ddot{\theta} + B_{44}(\dot{\theta})\dot{\theta} + C_{44}(\theta)\theta = 0 \quad (1)$$

where  $I_{44}$  is moment of inertia of ship that is a constant value.  $I_{44a}(\ddot{\theta})$  is non-linear added moment of inertia function.  $B_{44}(\dot{\theta})$  is non-linear damping moment function and  $C_{44}(\theta)$  is non-linear restoring moment function. In order to find non-linear functions, non-parametric system identification method is used.

Briefly, Pongdung's method [32] is chosen to determine non-linear functions because it able to find all non-linear functions in Equation 1 synchronously. The method needs measured motion data from free roll decay experiment or CFD (Computational fluid dynamics) to formulate inverse problem. Actually, the responses are outputs and are calculated via equation of motion that the non-linear functions of each term are known variable values. On the other hand, the responses become to input (measured data) in inverse problem and the non-linear functions become to output (unknown variables). Each moment terms are solved by inverse problem formalism and stabilized by Landweber's regularization method. Its solutions are chosen the optimal solution through L-curve criterion. Finally, the zero-crossing detection technique of measured data is compared with that solution for identifying each moment function and reconstruction them. For more detail can see in Pongdung et al. [32].

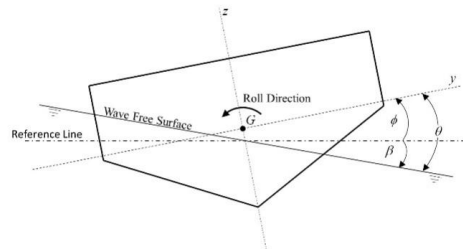


Figure 3. Rolling of ship on water wave free surface

When all non-linear functions is known, substituting

$\theta = \phi - \beta$  into Equation 1, it becomes

$$[I_{44} + I_{44a}(\phi - \beta)](\ddot{\phi} - \ddot{\beta}) + [B_{44}(\dot{\phi} - \dot{\beta})](\dot{\phi} - \dot{\beta}) + [C_{44}(\phi - \beta)](\phi - \beta) = 0 \tag{2}$$

Rearranging Equation 2, it yields

$$\begin{aligned} & [I_{44} + I_{44a}(\phi - \beta)]\ddot{\phi} + [B_{44}(\dot{\phi} - \dot{\beta})]\dot{\phi} \\ & + [C_{44}(\phi - \beta)]\phi = [I_{44} + I_{44a}(\phi - \beta)]\ddot{\beta} \\ & + [B_{44}(\phi - \beta)]\dot{\beta} + [C_{44}(\phi - \beta)]\beta \end{aligned} \tag{3}$$

Equation 3 is the full nonlinear ship motion: left-hand side is ship moment and right-hand side is exciting moment. The Equation 3 has the same coefficient function in the same term of inertia, damping and restoring: the roll angle and wave slope are equal values at steady state on time domain, but at transient are not.

Thus, define

$$\tau_w = [I_{44} + I_{44a}(\theta)]\ddot{\beta} + [B_{44}(\dot{\theta})]\dot{\beta} + [C_{44}(\theta)]\beta \tag{4}$$

The wave slope  $\beta$  is determined from Equation 5, which it is regular linear wave (deep water wave).

$$\eta(x, t) = \eta_0 \sin(kx - \omega t) \tag{5}$$

where  $\eta_0$  is wave amplitude,  $k$  is wave number,  $x$  is distance in  $x$  direction,  $\omega$  is angular frequency and  $t$  is time. When differentiate Equation 4 with  $x$ , it becomes to wave slope equation follow as Equation 6. Then wave slope velocity and acceleration are Equation 7 and 8 respectively.

$$\frac{d\eta(x, t)}{dx} = \beta = \eta_0 k \cos(-\omega t) \tag{6}$$

$$\dot{\beta} = \eta_0 k \omega \sin(-\omega t) \tag{7}$$

$$\ddot{\beta} = -\eta_0 k \omega^2 \cos(-\omega t) \tag{8}$$

Thus, a model for motion of the ship in roll together with and  $n$ -spinning-wheel gyro-stabilizer can be expressed follows as block diagram in Figure 4. Then it can be formulated in equation of motion follow as Equation 9 and 10.

$$I_{44} + I_{44a}(\theta)\ddot{\phi} + B_{44}(\dot{\theta})\dot{\phi} + C_{44}(\theta)\phi = \tau_w - \tau_g \tag{9}$$

$$I_g \ddot{\alpha} + B_g \dot{\alpha} + C_g \sin \alpha = \tau_s - \tau_p \tag{10}$$

where  $\alpha$ ,  $\dot{\alpha}$  and  $\ddot{\alpha}$  in Equation 9 are precession angle, precession rate and precession acceleration respectively. The following Equation 10  $I_g$ ,  $B_g$  and  $C_g$  are moment of inertia, damping and restoring coefficient of gyro-stabilizer about precession axis.

Equation 9 represents the full non-linear ship roll dynamics, while Equation 10 represents the non-linear dynamics of gyro-stabilizer about the precession axis. The following Equation 9 and Equation 10 associate coupled system, the wave-induce roll moment ( $\tau_w$ ) excite the ship rolling. When roll motion develops, the roll rate induces a moment about the precession axis of spinning wheels ( $\tau_s$ ). And then the spinning wheels develop precession, its reaction moment resists on the ship with opposes direction of the wave-induce moment ( $\tau_g$ ).

$$\tau_s = K_g \dot{\phi} \cos \alpha \tag{11}$$

$$\tau_g = nK_g \dot{\alpha} \cos \alpha \tag{12}$$

where  $K_g$  is spinning angular momentum ( $K_g = \omega_{spin} I_{spin}$ )

The roll stabilization moment for passive system can be modified the precession damping and stiffness as well as leave the gyro to free work. For an active system, it is controlled through the precession dynamics via the precession control moment that is PD controller and expressed follow

$$\tau_p = K_p \alpha + K_d \dot{\alpha} \tag{13}$$

where  $K_p$  is proportional control gain and  $K_d$  is derivative control gain. The advantage of this control law is no needing ship roll sensors.

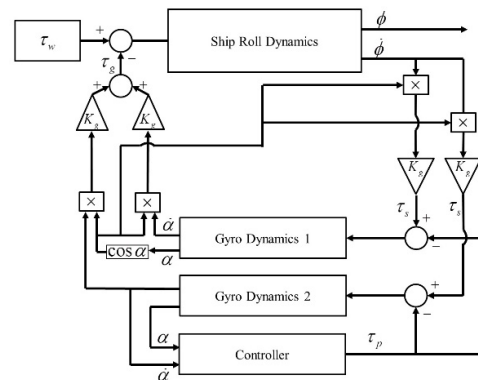


Figure 4. Block diagram of full non-linear twin gyro-stabilizer model

### 2.2 Linear Gyro-stabilizer Model

In the past, analysis any control systems via equation of motions were treated to be linear differential equation. There are reduced complexity and able to transform to s-domain, and then change s-domain to be frequency domain. At steady state, the analysis control systems through frequency domain are proper. This section uses almost equation from Perez and Steinmann (2009) [23]

From Equation 9 and Equation 10, the models are linearized: for small angle of roll and precession, the coefficients of left-hand side are constant value. However, let define,

$$\dot{\phi} \cos \alpha \approx \dot{\phi} \tag{14}$$

$$\dot{\alpha} \cos \alpha \approx \dot{\alpha} \tag{15}$$

and

$$\sin \alpha \approx \alpha \tag{16}$$

Hence, the linear equation expressed as follow:

$$(I_{44} + I_{44a})\ddot{\phi} + B_{44}\dot{\phi} + C_{44}\phi = \tau_w - \tau_g \tag{17}$$

$$I_g \ddot{\alpha} + B_g \dot{\alpha} + C_g \alpha = \tau_s - \tau_p \tag{18}$$

$$\tau_w = (I_{44} + I_{44a})\ddot{\beta} + B_{44}\dot{\beta} + C_{44}\beta \tag{19}$$

$$\tau_s = K_g \dot{\phi} \tag{20}$$

$$\tau_g = nK_g \dot{\alpha} \tag{21}$$

Note that,  $\tau_p$  no changes in linear model. And linear gyro-stabilizer system is demonstrated in Figure 5.

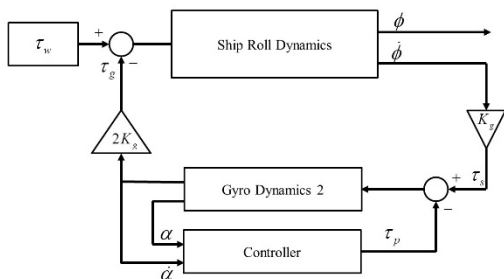


Figure 5. Block diagram linear twin gyro-stabilizer model

From zero condition, thus the open loop transfer function is

$$H_{ol}(s) = \frac{\phi_{ol}(s)}{\tau_w(s)} = \frac{1}{(I_{44} + I_{44a})s^2 + B_{44}s + C_{44}} \tag{22}$$

The close loop transfer function is

$$H_{cl}(s) = \frac{\phi_{cl}(s)}{\tau_w(s)} = \frac{I_g s^2 + B'_g s + C'_g}{(I_{44}s^2 + B_{44}s + C_{44})(I_g s^2 + B'_g s + C'_g) + nK_g^2 s^2} \tag{23}$$

where  $\phi_{ol}(s)$  and  $\phi_{cl}(s)$  are Laplace transforms open and close loop roll angle respectively. And the transfer function of precession angle to roll angle is

$$H_{pr}(s) = \frac{\alpha(s)}{\phi(s)} = \frac{\dot{\alpha}(s)}{\dot{\phi}(s)} = \frac{K_g s}{I_g s^2 + B'_g s + C'_g} \tag{24}$$

where

$$B'_g = B_g + K_d \tag{25}$$

$$C'_g = C_g + K_p \tag{26}$$

The transfer function of precession angle to wave exciting roll moment that is the result from Equation 23 and 24 is

$$H_{pw}(s) = \frac{\alpha(s)}{\tau_w(s)} = H_{pr}(s)H_{cl}(s) = \frac{K_g s}{(I_{44}s^2 + B_{44}s + C_{44})(I_g s^2 + B'_g s + C'_g) + nK_g^2 s^2} \tag{27}$$

Rearranging Equation 24, it yields

$$H_{pr}(s) = \left( \frac{K_g}{I_g} \right) \left( \frac{s}{s^2 + \frac{B'_g}{I_g} + \frac{C'_g}{I_g}} \right) \tag{28}$$

and the roots are

$$p_{1,2} = -\frac{B'_g}{I_g} \pm \sqrt{\left( \frac{B'_g}{I_g} \right)^2 - 4 \frac{C'_g}{I_g}} \tag{29}$$

Both roots are negative real roots (stability condition) if and only if,  $B'_g > 0$ ,  $C'_g > 0$  also constraint of

$$\left(\frac{B'_g}{I_g}\right)^2 > 4\frac{C'_g}{I_g} \tag{30}$$

The following Equation 13, the proportional term is set during design due to centre of mass location, normally locate below the precession axis, which like a pendulum, the  $C'_g$  value is fixed. Thus, the control moment becomes

$$\tau_p = K_d \dot{\alpha} \tag{31}$$

From Equation 30, it able to formulate the condition of two poles to be real root:

$$B'_g > \sqrt{4C'_g I_g} \tag{32}$$

It can set as

$$B'_g = \gamma \sqrt{4C'_g I_g}, r > 1 \tag{33}$$

Then substitute Equation 33 in to Equation 25, it become

$$K_d = \gamma \sqrt{4C'_g I_g - B_g}, r > 1 \tag{34}$$

This derivative control gain is used through under constrained performance follow section 2.4

### 2.3 Control Performance and Limitations

In order to observe the objective performance, the output sensitivity function is defined as:

$$S(s) \triangleq \frac{\phi_{cl}(s)}{\phi_{ol}(s)} \tag{35}$$

The Bode's integral constraint is

$$\int_0^{\infty} \log |S(j\omega)| d\omega = 0 \tag{36}$$

and the roll reduction (complementary sensitivity function) is defined as

$$RR(\omega) = 1 - |S(j\omega)| = \frac{|\phi_{ol}(j\omega)| - |\phi_{cl}(j\omega)|}{|\phi_{cl}(j\omega)|} \tag{37}$$

the integral constrain becomes

$$\int_0^{\infty} \log |1 - RR(j\omega)| d\omega = 0 \tag{38}$$

Another form of roll reduction function is

$$RR(\omega) = \left(1 - \frac{|H_{cl}(j\omega)|}{|H_{ol}(j\omega)|}\right) \tag{39}$$

Note that, the roll reduction values possible to be negative or positive values but less than 1 along interested range of frequency. The meaning of negative value is roll amplification. The meaning of positive value is roll reduction. Then the roll reduction close to 1, it has better performance.

### 2.4 Constrained Performance

The additional constrain is cause by the precession angle limiting due to mechanical design. If the precession angle reaches this limit, the device may get damage or deteriorate. Additionally, it may causes of roll amplification rather than roll reduction of ship: phase of resisting moment cannot eliminate wave induce roll moment.

For a regular wave of frequency  $\omega^0$  and wave height  $H_s^0$ , it induces roll exciting moment amplitude  $\tau_w^0$ . The following Equation 27, it can be obtained the amplitude of precession angle:

$$\bar{\alpha}^0 = |H_{pw}(j\omega^0)| \bar{\tau}_w^0 \tag{40}$$

The given constrain is the maximum precession angle  $\alpha_{max}$ , it can be obtained the optimal of  $B'_g$  that it take the precession angle close to its limit:

$$\gamma^*(\omega^0) = \arg \min_{\gamma > 0} \left| \alpha_{max} - \left| H_{pw}(j\omega^0, B'_g(\gamma)) \right| \bar{\tau}_w^0 \right| \tag{41}$$

### 3. Cases Study Configurations and Numerical Experiment Setup

To carry out the aim of this presentation, the non-linear gyro-stabilizer system is validated with linear gyro-stabilizer system to observe and analyze its performance at the same environment and limitation. The vessel was set to zero speed and moved against beam sea direction. In order to determine the system design point, assume that the system was designed for deep water wave, significant wave height of 0.04 m, all frequency of its.

In order to observe and analyze non-linearity of a gyro-stabilizer system, this present, V-hull section was selected because it is a general section profile of high-speed boat and small ship that are suited. The dimensions of selected V-hull are demonstrated in Figure 6. Both linear and non-linear equation of motion was found via

measured data that were the result from CFD method, XFLOW commercial program. The simulations are set to be unsteady flow. There is free roll decay method, which was set initial condition of roll angles are 5, 10, 15, 20, 25 and 30 degrees. According to CFD simulation results, the example of measured data from simulation case, which was set 30 degree of initial condition was demonstrated in Figure 7.

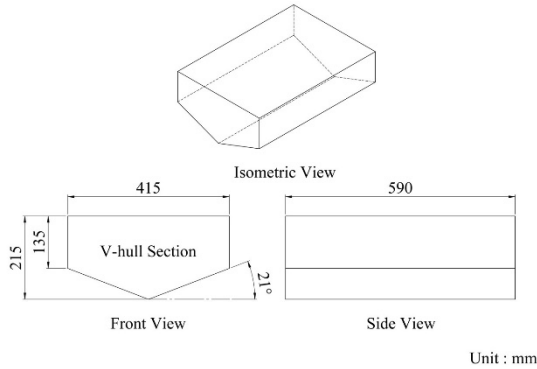


Figure 6. The V-hull Geometry and dimension for simulation

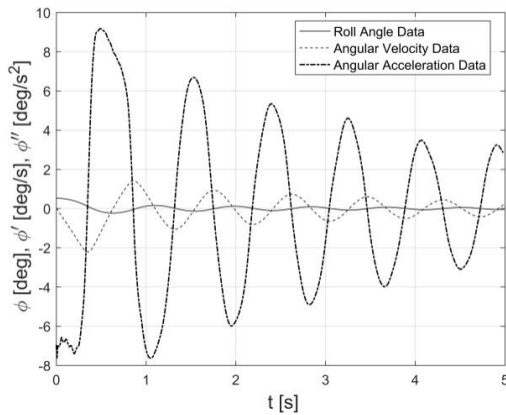


Figure 7. Measured Data from CFD of Initial Condition 30 Degree

The linear ship model was formulated from logarithmic decrement method. The method appropriates to small roll motion less than 8 degree. It requires only roll angle data (measured data from CFD) to detect maxima or minima values, where are used to find estimated exponential function. The function leads to determine the damping ratio and natural frequency. There can be converted to add moment of inertia, damping coefficient. However, restoring coefficient can be found from inclination calculation. According to this method, the details of calculation were omitted in this presentation.

For this paper, the simulation of 5 degree of initial condition was used. The estimating of exponential function was shown on Figure 8. According to estimated exponen-

tial function the linear ship model is

$$0.3255\phi + 0.0494\dot{\phi} + 19.7321\ddot{\phi} = 0 \tag{42}$$

Note that, in free roll motion test  $\theta = \phi$ , there are not have relative motion between free surface and roll motion angle and  $I_{44} = 0.26$ .

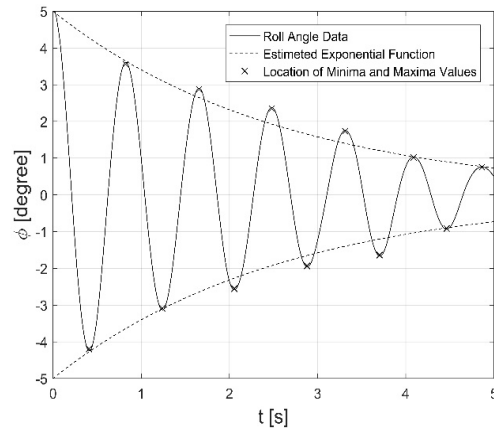


Figure 8. Determination of exponential function from roll angle data of 5 degree initial condition

The non-linear ship model was formulated by reconstruction non-linear damping coefficient and added moment of inertia via systems identification method that used all of measured data (roll angle, angular velocity and angular acceleration) and all initial condition from CFD method.

The non-linear restoring coefficient function was known via inclination calculation. The calculation result was fitted by polynomial function follow as Equation 43 and its curve was shown at the top of Figure 9.

$$C_{44}(\phi) = -19.7321\phi^{18} + 108.8680\phi^{16} - 258.2096\phi^{14} + 344.3239\phi^{12} - 283.2101\phi^{10} + 148.2937\phi^8 - 49.4689\phi^6 + 10.4220\phi^4 - 1.4402\phi^2 + 0.1454 \tag{43}$$

The non-linear damping coefficient function was found by accumulating the damping moment data point from system identification method, and there were taken by curve fitting method which is shown in the middle of Figure 9. Then the moment function was divided by  $\phi$ , thus the non-linear damping coefficient is

$$B_{44}(\dot{\phi}) = 0.1588\dot{\phi}^2 + 0.1391 \tag{44}$$

From the same procedure of formulating non-linear damping moment, the added moment of inertia fitting curve is shown at the bottom of Figure 9 and its average

value is

$$I_{44a} \left( \ddot{\phi} \right) = 0.066 \quad (45)$$

The full non-linear ship model was simulated on free decay motion with 30 degree initial condition to verify its accuracy. The simulated result of roll angle via Equation 1 was plotted in Figure 10 also result from linear model and measured roll angle from CFD. It proves that the non-linear model is better accuracy more than linear model, when both results were compared with measured roll angle from CFD. Hence, the non-linear ship model has enough accuracy and can be used in this presentation.

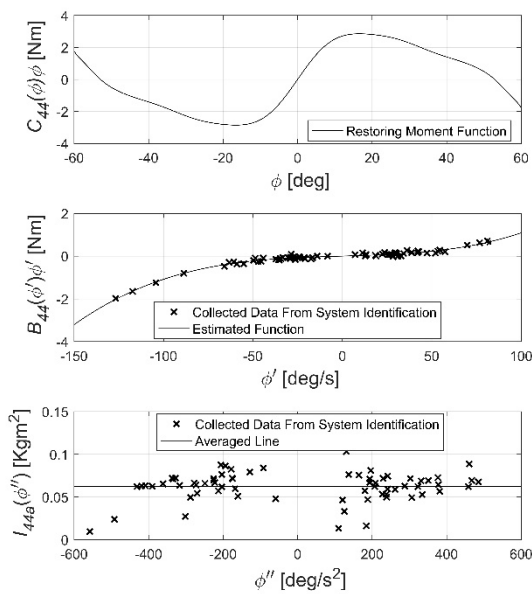


**Figure 9.** The Estimating functions of restoring moment (top), damping moment (middle) and added moment of inertia (bottom)

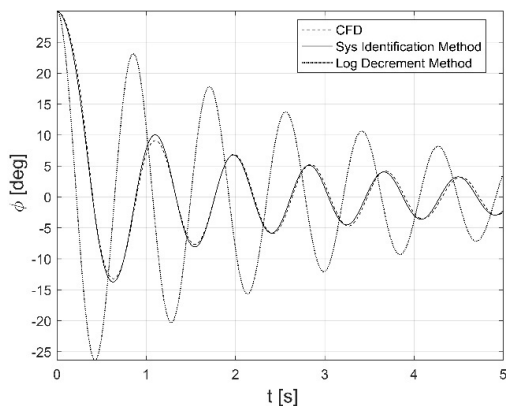


**Figure 10.** The comparison of simulations between results of non-linear ship model (system identification method) and linear ship model (logarithmic decrement method) with measured data from CFD

The non-linear and liner gyro-stabilizer model was used according to Equation 10 and Equation 18 respectively. There have same characteristic coefficients. The gyro-stabilizer was assumed that its speed is constant at 300 rpm ( $\omega_{spin}$ ), the moment of inertia about spin axis is  $0.0125 \text{ kg}\cdot\text{m}^2$  ( $I_{spin}$ ) and the moment of inertia about precession axis is  $0.0005 \text{ kg}\cdot\text{m}^2$  ( $I_g$ ). The damping coefficient is zero  $B_g = 0$ , there is on friction about precession axis. The restoring coefficient is zero; the center of gravity position was located at middle of spin and precession axis (no effect of pendulum).

The following Equation 13, the proportional gain  $K_p$  is fixed value of 0.1. The derivative gain was determined via Equation 34 and Equation 41.

Both linear and non-linear systems were determined through frequency domain and simulated with regular waves, which the range of frequencies is 0 to 14.84 rad/s. The simulation cases of linear system were varied wave amplitudes from  $\eta_0 = 0.02 \text{ m}$  up to  $1.5\eta_0$ . The linear simulation case of  $\eta_0$  was set to be reference case. The  $\gamma^*$  of each wave amplitude of simulation cases follow Equation 41 were gathered, and then they were used in simulation cases of full non-linear system. The full non-linear system was simulated in time domain with only amplitude of  $\eta_0$ . Moreover, in order to find a design trade-off, the  $\gamma^*$  of each wave amplitude of linear system were used. The name of simulation cases are described in Table 1.

**Table 1.** The description of simulation cases

| Case Name          | Description  | Gyro-model | Ship-model |
|--------------------|--|------------|------------|
| LSOL               | Linear open loop system  | -          | Linear     |
| LSCL               | Linear close loop system   | Linear     | Linear     |
| LSCL @ $c\eta_0$   | Linear close loop system that determined with wave amplitudes of $c\eta_0$ ( $c=1.1, 1.2, 1.3, 1.4$ and $1.5$ )                  | Linear     | Linear     |
| FNSOL              | Full non-linear open loop system   | -          | Non-linear |
| FNSCL              | Full non-linear close loop system  | Non-linear | Non-linear |
| FNS-CL @ $c\eta_0$ | Full non-linear close loop system with the $\gamma^*$ values of each wave amplitude of LSOL ( $c=1.1, 1.2, 1.3, 1.4$ and $1.5$ ) | Non-linear | Non-linear |

### 4. Results and Discussions

In order to examine the characteristics of performances of non-linear gyro-stabilizer system, the linear system was determined first. The following Figure 11 – 14, they show the results of linear gyro-stabilizer characteristics.

Figure 11 show exciting moment (input), the result from Equation 19. The graph was also plotted Stokes limit; the exciting moment cannot exceed this line at upper

side. Stokes and exciting moment line of amplitude 0.02 m intersect at 14.84 rad/s, which it was set to be maximum value of frequency range. All lines have tough at  $\omega = 7.786$  rad/s that is natural frequency of linear vessel model because it has the same coefficients. And then, when frequencies increase, the exciting moment rapidly increase. It is obviously the increasing of wave amplitudes correspond to increasing exciting moment.

Figure 12 and 13 are they were  $\gamma^*$  values and precession angles of each wave amplitude respectively. They simultaneously determined via Equation 27 and 41.

Figure 12 shows the minimum  $\gamma^*$  values of each wave amplitude. All wave amplitudes gave  $\gamma^*$  values of 1 until the system gets the exciting frequency that makes the precession angle reach its limit value (60 degree, also observe Figure 13). It has been called critical point. From this point  $\gamma^*$  value rapidly increasing to keep precession angle does not exceed 60 degree. As the higher wave amplitude, the critical points have appeared at lower frequency.

Figure 13 shows the precession angles in frequency domain. The trend of precession angle resembles the pose of exciting moment in Figure 11. However, the crests of all lines about exciting frequency value of 2 were affected from turning proportional gain  $K_p$  that was fixed value of 0.1. And the higher wave amplitude gives the higher precession angle. The flat band at high exciting frequency that has constant value of 60 degree is explained as above paragraph.

Figure 14 shows the roll angle responses. At the lower exciting frequency from critical point, the result trends resemble precession angle but it rapidly increases when the exciting frequency increase from critical point. The increasing rapidly of roll angle from the critical point is caused by the precession angle reach its limit, which it cannot have more precession rate to create resisting moment for cancel exciting moment. Moreover, at the higher wave amplitude gives the higher roll angle response.

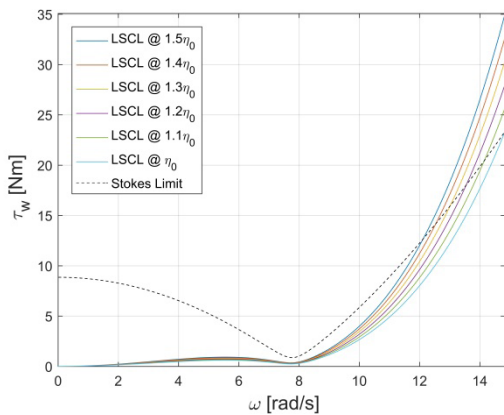


Figure 11. Exciting moment of the linear gyro-stabilizer model

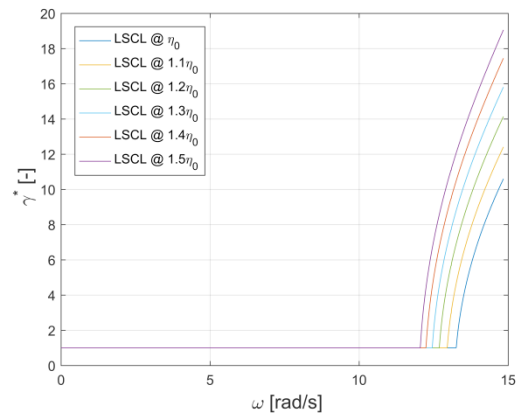


Figure 12. Estimating of  $\gamma^*$  values each wave amplitude from Equation 41

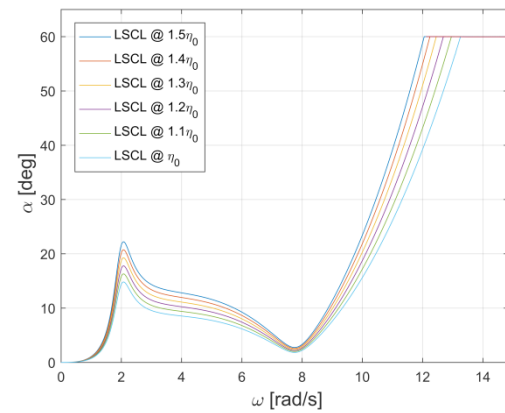


Figure 13. Precession angles of linear gyro-stabilizer model so that determined via Equation 27 and 41 with the following  $\gamma^*$  values each wave amplitude in Figure 12

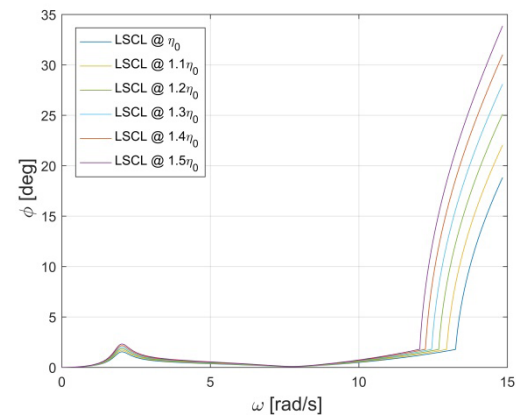


Figure 14. Roll angle responses of linear gyro-stabilizer model each wave amplitude via Equation 23

The following linear model results consistent and reasonable to each other. They can be used to compare with the non-linear system in the same wave condition. How-

ever, according to section 3, the non-linear gyro-stabilizer system model was assumed as it was designed to operate in beam sea that it has significant wave height ( $H_{1/3}$ ) of 0.04 m ( $\eta_0 = 0.02$  m). But it cannot directly determine  $\gamma^*$  through transfer function like linear system model. Thus the  $\gamma^*$  values each wave amplitude from linear model were applied to non-linear model. The non-linear system needs to simulate in time domain and collected the amplitude simulation results at steady state. Hence, Figure 15 - 18 illustrate the comparison between linear and non-linear model. Some data of non-linear model disappear because of its solutions became unstable (no steady state) when the precession angle reached the limit angle.

Figure 15 shows the exciting moments both open and close loop of linear and non-linear system. They have the trend like exciting moments of linear system. Linear open loop and close loop exciting moments are same line because they have same coefficients of vessel model. The all non-linear exciting moment lines are above liner exciting moment at high frequencies from around the natural frequency. The difference of exciting moment values causes of the coefficient functions follow as Equation 4 that related to  $\theta$ ,  $\dot{\theta}$  and  $\ddot{\theta}$ .

Figure 16 shows the precession angle result that all non-linear precession angles have the same line until they reach to a limited angle at the exciting frequency value of 11.85 rad/s. And almost values are above linear system. The cause of all non-linear precession angles has the same values. They used same  $\gamma^* = 1$  as following Figure 12. After they reach the limited angle at higher frequencies, the data lost because the system became unstable so that it now has steady state. However, the non-linear system back to stable at the end of lines because of the increasing of  $\gamma^*$  value (see Figure 12) able to reduce the precession angles below limited angle. And then, they obviously show the higher  $\gamma^*$  each wave amplitude gave lower precession angle at the higher frequencies.

The following Figure 17, roll angle responses of the open and closed-loop of linear and non-linear systems are shown. The comparison between open-loop of linear and non-linear system obviously difference behavior along frequencies range; the linear open-loop system is fair curve, while the non-linear closed-loop system has the apex at the frequency value of 6 rad/s. This is the important cause to deep studying throughout non-linear gyro-stabilizer system; a difference response behavior will give the difference a system design point. The linear and non-linear closed-loop systems have a same trend. All non-linear roll angle responses have same values until they reach the frequency of 11.85 rad/s and almost

roll angle responses values are above the linear line. The closed-loop non-linear system uses more precession angle than linear system but they give more roll angle responses than linear system. After the critical point of linear closed loop system, all lines of roll angle responses increase and approach to open-loop systems because precession angles were forced and reduced to constant in linear model and non-linear model respectively. This reason refers to inefficiency of the systems, when the precession angle reaches the limited angle.

Figure 18 explains the responses in view of a relative roll angle response and can say that are the inverse behavior of a roll angle response. While the stabilizer attempt to keep roll angle approach to zero, the difference between a wave slope and roll angle increase (see relation in Figure 3).

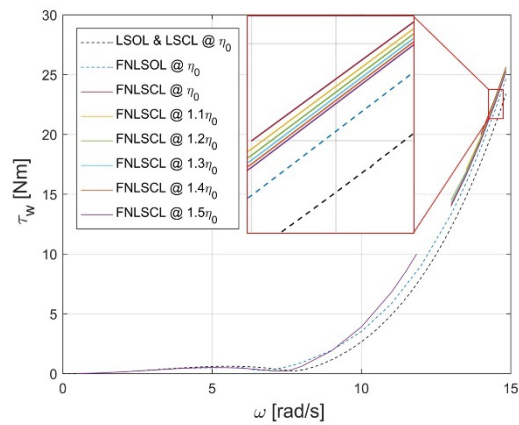


Figure 15. Comparison exciting moments between non-linear and linear gyro-stabilizer models; the linear model of  $\eta_0$  was set to be the reference

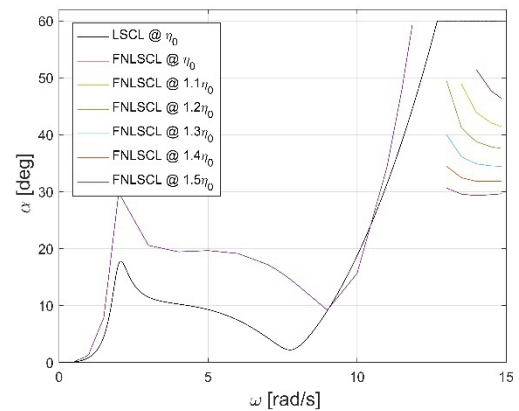
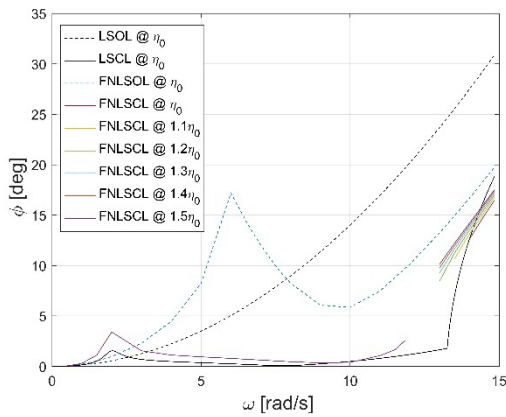
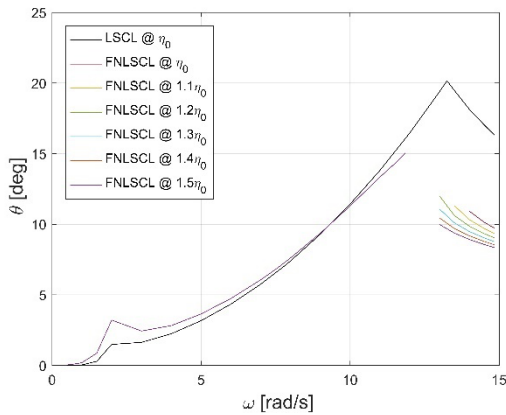


Figure 16. Comparison precession angle responses between non-linear and linear gyro-stabilizer models; the linear model of  $\eta_0$  was set to be the reference



**Figure 17.** Comparison roll angle responses between non-linear and linear gyro-stabilizer models; the linear model of  $\eta_0$  was set to be the reference



**Figure 18.** Comparison relative roll angle responses between non-linear and linear gyro-stabilizer models; the linear model of wave amplitude  $\eta_0$  was set to be the reference

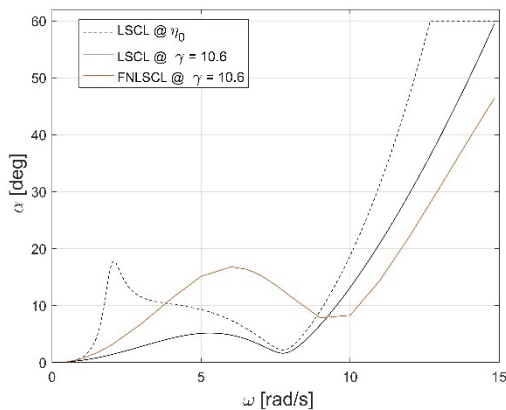


**Figure 19.** Precession angle responses of linear and non-linear gyro-stabilizer model of wave amplitude  $\eta_0$  and fix  $\gamma = 10.6$

The non-linear behaviors were analysed and explained throughout frequency domain as they were mentioned above. However, in reality, a  $\gamma^*$  value cannot adjust base on frequency domain as following Figure 12; a frequency cannot know immediately in time domain. Thus a  $\gamma^*$  will be selected only one value from Figure 12 so that appropriate with operation requirements. The  $\gamma^*$  value of 10.6 was selected. It locates at the right end of line LSCL @  $\eta_0$ . The value is the highest value, which forces the precession angle to work do not exceed the limited angle throughout the frequency range. Then the selected value was used for both linear and non-linear gyro-stabilizer system. The results were plotted follow as Figure 19 - 22 in frequency domain. In order to examine the effect of non-linearity, linear and non-linear gyro-stabilizer system model were simulated in irregular wave model of Bretschneider's [34] method that it has significant wave height of 0.04 m and the results were plot in Figure 23.

The following Figure 19, the precession angles of non-linear system work under the limited angle throughout frequency range. It has same characteristic of linear system but has different values. Hence, the roll angle response in Figure 20 is consequence of precession angle. The roll angle response of non-linear system has same characteristic of linear system but has different values as well.

Figure 21 shows the frequency response results. The peak of frequency response of non-linear open-loop system that refers to the natural frequency of vessel is different from linear open-loop system. The curve of linear closed-loop system is fair curve and approach to zero throughout the frequency range. The curve of non-linear closed-loop system has same behaviour of open-loop and its peak is lower. According to Figure 22, the reduction rates of linear and non-linear system are shown. The reduction rate refers to the efficiency of the stabilizer system. The non-linear system has the reduction rate values near linear system at the frequencies lower than 6 rad/s. But at the higher frequencies value, the reduction rate values of non-linear system are lower.

According to the previous results, the  $\gamma^*$  value was selected and fixed. They are made to clearly understand and proved that the non-linearity of non-linear model give a lot of different results at all. Thus, the designing base on linear model may give the wrong respond in reality. In order to prove again, the linear and non-linear gyro-stabilizer system models were simulated in same irregular beam sea on time domain. Assume that, precession angle is limited by mechanism at 90 degree but the  $\gamma^*$  value was selected from the limited angle at 60 degree of regular wave amplitude in order to let it has margin to prevent a

damage when the gyro-stabilizer system get higher amplitude in irregular wave.

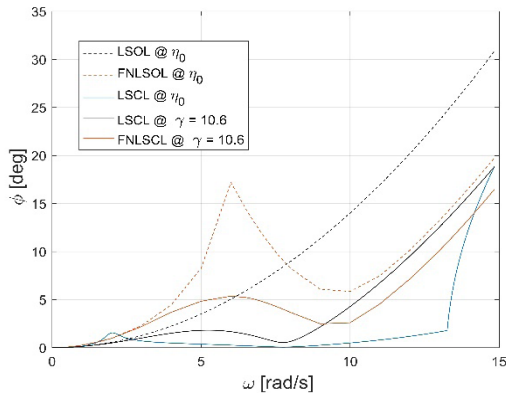


**Figure 20.** Roll angle responses of open and close loop condition of linear and non-linear gyro-stabilizer model of wave amplitude  $\eta_0$  that the close loop model was set the fix value of  $\gamma = 10.6$

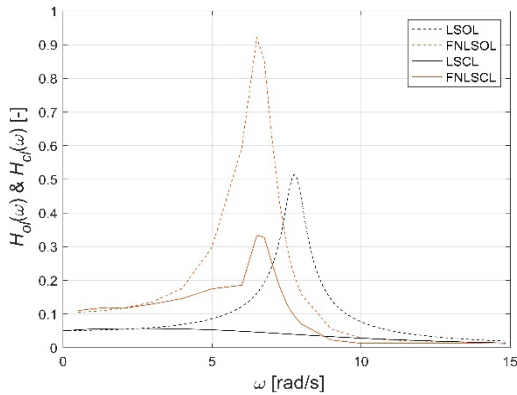


**Figure 21.** Comparison of frequency responses of open and close loop condition of linear and non-linear gyro-stabilizer model of wave amplitude  $\eta_0$  that the close loop models were set the fix value of  $\gamma = 10.6$

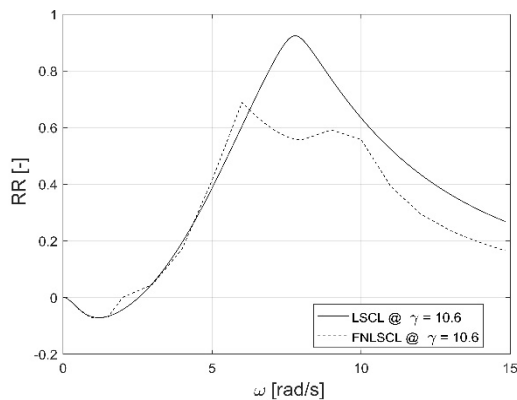


**Figure 22.** Comparison of reduction rate between linear and non-linear gyro-stabilizer model of wave amplitude  $\eta_0$  that the close loop models were set the fix value of  $\gamma = 10.6$

In the following Figure 23, the setting of gyro-stabilizer simulation cases (linear and non-linear system) were simulated in irregular wave model. The gyro-stabilizers were switched off first, and then begin to switched on at 20 second of simulation time to observe the difference of behaviors when the gyro-stabilizer models were switch off and on. The systems performances were gathered and shown in Table 2 in root mean square. At the top of Figure 23, the exciting moments of linear and non-linear system were shown. They were induced from the same irregular wave model but it gave exciting moment amplitude and phase shift slightly difference. The RMS of exciting moment of linear model has the value less than non-linear model so that accord to Figure 15. When the stabilizer switched off, the vessel did not stabilize. The roll angle response of linear model shown at the middle of Figure 23 has the RMS value more than non-linear model slightly. These results accord to Figure 20. When the gyro-stabilizers were switched on, the precession began to move for stabilize the vessel, the roll angle responses were reduced. The precession angle responses were shown at the bottom of Figure 23. As the gyro-stabilizer switched on, the precession angle of linear model has RMS value more than non-linear accord to Figure 19. And the roll angle response of linear model has RMS value lower than non-linear model. However, the reduction rate (RR) of linear system has RMS value more than non-linear system and so very different.

As the mentioned these results, they clearly show that the designing via the linear model cloud makes the gyro-stabilizer system miss the design point of mission requirements. On the other hand, the non-linear system model cloud gives more approach to reality for designing follow mission requirements.

**Table 2.** The root mean square values (RMS) of gyro-stabilizer system performances in irregular beam sea according to Figure 23; the significant wave height and average wave frequency is 0.04 m and 10.68 rad/s respectively.

| Model  | $\tau_w$ [Nm] | $\alpha$ [deg] | $\phi$ [deg] | RR [-] |
|--------|---------------|----------------|--------------|--------|
| LSOL   | 14.5          | -              | 21.56        | -      |
| FNLSOL | 15.38         | -              | 18.57        | -      |
| LSCL   | 14.5          | 32.03          | 4.75         | 0.78   |
| FNLSCL | 15.05         | 31.13          | 11.46        | 0.38   |

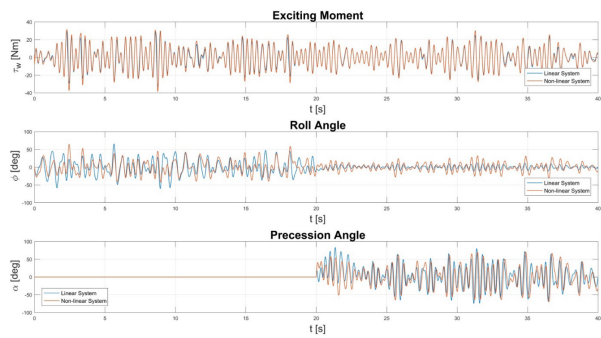


**Figure 23.** Comparison of linear and non-linear gyrostabilizer system model when they are switched off and on in irregular wave with  $\gamma = 10$ .

## 5. Conclusions

A gyro-stabilizer is the interesting system that it can apply to marine vessels for diminishes roll motion. Today it has potentially light weight with no hydrodynamics drag and effective at zero forward speed. The twin-gyroscope was chosen for this presentation because of it not has side effect moment. Almost, the modelling for designing the system use linear model that it might not comprehensive mission requirement such as high sea condition (high wave amplitude and various frequencies). Thus, the non-linear model becomes important role because it able to give the interested results approach to reality more than linear model. The non-linearity analysis was proved by comparison the results between linear and non-linear model of gyro-stabilizer throughout frequency domain also same wave input, constrains and limitations. Moreover, they were cross-checked by simulating in time domain.

Actually, controller gains of the non-linear model cannot directly determine the appropriated turning gain  $K_d$  via frequency domain analysis. Hence the  $K_d$  of non-linear model was approximated by selecting the  $\gamma^*$  value so that resulted to  $K_d$  from linear model at the highest frequency value of selected wave amplitude. The comparison of interested results as wave exciting moment  $\tau_w$ , precession angle  $\alpha$ , roll angle response  $\phi$  and reduction rate of linear and non-linear close loop model in frequency domain has demonstrated the similar characteristics but gave different values at same frequency obviously. The results were confirmed again by simulation in irregular beam sea on time domain and they demonstrate the difference of behavior of both systems while the gyro-stabilizer was switching on and off.

From the resulting analysis, the non-linear gyro-stabilizer model gives the results closer to realistic that correspond to more accuracy in a designing gyro-stabilizer control system for various amplitudes and frequencies

operating condition especially high sea condition.

## References

- [1] Chadwick, J.H. (1955), "On the stabilization of roll", *Trans. Soc. Naval Arch. Marine Eng*, 63, 237-280.
- [2] Marzouk, O.A. and Nayfeh, A.H. (2009), "Control of ship roll using passive and active anti roll tanks", *Ocean Engineering*, 36(9), 661-671.
- [3] Haghghi, H. and Jahed-Motlagh, M.R. (2012), "Ship roll stabilization via Ssliding mode control and gyrostabilizer", *Bul. inst. politeh. iai Autom. control Comput. sci. sect. J*, 1, 51-61.
- [4] Townsend N.C., Murphy, A.J. and Sheno, R.A. (2007), "A New Active Gyrostabiliser System for Ride Control of Marine Vehicles". *Ocean Engineering*, 34 (11-12), 1607-1617.
- [5] Lewis, V.E. (1986), "Principles of Naval Architecture". The Society of Naval Architects and Marine Engineers. Chapter IX.
- [6] Lloyd, A.R.J.M. (1998), "Seakeeping Ship Behaviour in Rough Weather". Ellis Horwood Ltd.
- [7] Brennan, L. (1905), "Means for Imparting Stability to Unstable Bodies", US Patent 796893.
- [8] Sperry, E.A. (1908), "Steadying device for vehicles", Patent US 907907.
- [9] Schilovski, P.P. (1909), "Gyrocar", Patent GB 12021.
- [10] Schilovski, P.P. (1914), "Gyrocar", Patent GB 12940.
- [11] Beznos, A.V., Formal'sky, A.M., Gurfinkel, E.V., Jicharev, D.N., Lensky, A.V., Savitsky, K.V. and Tchesalin, L.S. (1998). "Control of autonomous motion of two-wheel bicycle with gyroscopic stabilization", *Proceedings—IEEE International Conference on Robotics and Automation* 3, 2670-2675.
- [12] Karnopp, D. (2002), "Tilt control for gyro-stabilized two-wheeled vehicles". *Vehicle System Dynamics*, 37 (2), 145-156.
- [13] Brown, H.B., Jr. and Xu, Y. (1996), "A Single-Wheel, Gyroscopically Stabilized Robot", *Proc. of the 1996 IEEE Int. Conf. on Rob. And Autom*, Minneapolis, Minnesota.
- [14] Aubrun, J.N. and Margulies, G. (1979). "Gyrodampers for large scale space structures", *Technical Report*, NASA CR-159 171.
- [15] Woolsey, C.A. and Leonard, N.E. (2002), "Stabilizing underwater vehicle motion using internal rotors", *Automatica*, 38 (12), 2053-2062.
- [16] Schultz, C. and Woolsey, C.A. (2003), "An experimental platform for validating internal actuator control strategies", In: *IFAC Workshop on Guidance and Control of Underwater Vehicles*, April 2003, Newport, South Wales, UK, 209-214.
- [17] Sperry, E.A. (1910), "The gyroscope for marine pur-

- poses”, Transactions of the Society of Naval Architects and Marine Engineers XVIII, 143-154.
- [18] Schlick, E.O. (1904a), “Device for minimising the oscillatory movements of ships”, Patent US 769493.
- [19] Schlick, E.O. (1904b), “The gyroscopic effect of fly-wheels on board ship”, Transactions of the Institute of Naval Architects, 23, 117-134.
- [20] Forbes, T.C. (1904), “Device for steadying ships” Patent US 769693.
- [21] Sperry, E.A. (1908), “Steadying Device for Vehicles”, Patent US 907907.
- [22] McGookin, M., Anderson, D. and McGookin, E. (2008), “Application of MPC and sliding mode control to IFAC benchmark models”. In: UKACC International Conference on Control 2008, Manchester, UK.
- [23] Perez, T. and Steinmann, P. D. “Analysis of Ship Roll Gyrostabilizer Control”, Proceedings of the 8th IFAC International Conference on Manoeuvring and Control of Marine Craft, Guarujá (SP), Brazil.
- [24] Masri, S.F., Chassiakos, A.G. and Cauchey, T.K. (1993), “Identification of nonlinear dynamic systems using neural networks”, Journal of Applied Mechanics. 60(1), 123-133.
- [25] Chassiakos, A.G. and Masri, SF (1996), “Modeling unknown structural systems through the use of neural network”, Earthquake Engineering & Structural Dynamics, 25(2), 117-128.
- [26] Liang, Y.C., Zhou, C.G. and Wang, Z.S. (1997), “Identification of restoring forces in non-linear vibration systems based on neural networks”. Journal of Sound and Vibration. 206(1), 103-108.
- [27] Liang, Y.C., Feng, D.P. and Cooper, J.E. (2001), “Identification of restoring forces in non-linear vibration systems using fuzzy adaptive neural networks”. Journal of Sound and Vibration. 242(1), 47-58.
- [28] Jang, T.S., Kwon, S.H. and Han, S.L. (2009), “A novel method for non-parametric identification of nonlinear restoring forces in nonlinear vibrations from noisy response data: A conservative system”, Journal of Mechanical Science and Technology. 23(11), 2938-2947.
- [29] Jang, T.S., Kwon, S.H. and Lee, J.H. (2010) “Recovering the functional form of the nonlinear roll damping of ships from a free-roll decay experiment: An inverse formulism”, Ocean Engineering. 37, 14-15.
- [30] Jang, T.S. (2011), “Non-parametric simultaneous identification of both the nonlinear damping and restoring characteristics of nonlinear systems whose dampings depend on velocity alone”, Mechanical Systems and Signal Processing. 25(4), 1159-1173.
- [31] Jang, T.S., Baek, H., Choi, S.H. and Lee S. (2011), “A new method for measuring nonharmonic periodic excitation forces in nonlinear damped systems”, Mechanical Systems and Signal Processing. 25(6), 2219-2228.
- [32] Pongduang, S., Chungchoo, C. and Iamraksa, P. (2020), “Nonparametric Identification of Nonlinear Added Mass Moment of Inertia and Damping Moment Characteristics of Large-Amplitude Ship Roll Motion”, Journal of Marine Science and Application, 19(2), 17-27.
- [33] Arnold, R.N. and Maunder, L. (1961), “Gyrodynamics and its Engineering Applications”, Academic Press, New York and London.
- [34] Bretschneider, C.L. (1959), “Wave variability and wave spectra for win-generated gravity waves”, Technical Memorandum No. 118, Beach Erosion Board, U.S. Army Corps of Engineers, Washington, DC, USA.